Chapter 1 Electrostatic Fields at Protein-Protein Interfaces: Increased Sampling Time and Various Electrostatic Methods: A Case for Simulating in Polarizable Force Fields

1.1 Introduction

One of the principle grievances with PB electrostatics is the arbitrary choice of solute dielectric. In fact, it can be trivially shown that the solute dielectric is just a scaling factor and can be adjusted *ex post facto* to force the calculated field values to yield experimental Stark shifts consistent with the known Stark tuning rate. While this may be beneficial from the stance of a machine learning algorithm where the relationship is the most important factor and the physics are just an afterthought, it is unsatisfying for trying to predict fields of new or interesting molecules. In fact, it is my opinion that the ideal use of these calculations would be to calculate the field in regions of biological molecules which do not contain, and therefore are not perturbed (no matter how slightly), by a VSE probe. This would allow for targeted drug design on biologically active biomolecules which are not dependent on assumptions about a probe's degree of perturbation. Unfortunately, for the model to work thusly we need to be significantly more confident in physical veracity of them. To do this, we need to remove assumptions about protein dielectrics.

A dielectric constant is a macroscopic bulk property describing the atomic polarizability of a material. At the atomic level, however, a dielectric constant is a relatively meaningless quantity that acts to indiscriminately screen electric charge. Water is known to have a relatively high dielectric of 78-80 at 298 K. This high dielectric is a result of each water molecule's ability to rearrange is orientation in response to the local electrostatic field. This rearrangement aligns its dipole moment parallel to the electrostatic field, resulting in an electrostatic field produced by the water molecule which is antiparallel to the local electrostatic field, reducing the sum electrostatic field, and therefore screening it for any atom further from the field source than that water

molecule. In contrast, a protein interior is significantly limited in the rotational degrees of freedom of sidechains, and therefore has less-capable of reorienting in response to a local electrostatic field. This results in a lower effective dielectric constant and less charge screening. Protein sidechains *can*, however, respond to a local field via an induced dipole moment, which has the same effect as rotating a permanent dipole moment and reducing the effect field further from the source. Conventional point charge force fields cannot account for the induced dipole moments directly, which has led us to the polarizable AMOEBA force field.

In this work we examine a variety of classical field calculation methods: RFM PB in Amber03 with a 10^3 Å^3 second-stage box and 193 grid points in each dimension, 5 Å explicit water sphere also with a 10^3 Å^3 second-stage box and 193 grid points in each dimension, explicit TIP3P using GROMACS reaction field electrostatics, hybrid solvent reaction field electrostatics and solute coulomb field, AMOEBA with PB solvent, and AMOEBA with explicit solvent. In both AMOEBA field methods, we also look at adding in charge-penetration via the fitted charge-penetration and the intuitive charge-penetration parameters previously described. In total, we performed 10 different electrostatic field methods.

In addition to examining a variety of classical electrostatic field models, we significantly increased the simulation time for each 2D Umbrella window from 0.4 ns to 2.0 ns each, for a total of 288 ns for each system. Furthermore, in addition to the Rap GTPases previously studied, we have also included simulations on Ras D30/E31, Ras D30E/E31, Ras D30/E31K, and Ras D30E/E31K, each bound to each of the six previously discussed nitrile probes. In total 54 different systems were each simulated for 288 ns, resulting in 15,552 total ns of simulation.

In this discussion, all references to APBS are using the RFM.

1.2 RESULTS AND DISCUSSION

Each electrostatic field method was plotted against the experimental vibrational absorption frequencies for the appropriate systems and the resulting correlation coefficients and virtual Stark tuning rates have been tabulated in Table 1-1.The table has been broken up into three sections: a single GTPase mutation, indicated in the leftmost column, and all of the probes it could be docked to; a single probe, indicated in the leftmost column, and all of the GTPase systems it could be docked to (including the undocked, monomeric stat); all 54 systems, indicated by "All Points". Each major column shows a different electrostatic method. Changed in electrostatic field due to the monomer docking to each GTPase system is tabulated in Table 1-2, where the data is presented in the same manner as Table 1-1. The case where a single probe location is measured when docked to each GTPase is excluded because all the results would be shifted by a constant amount--whatever the particular shift and calculated field is for the monomeric probe.

1.2.1 Electrostatic Fields Along the Interface of Each GTPase

First we examine how well a single mutation is seen at different points along the Ral surface by comparing the field calculated at each probe site when docked to the same GTPase. Moving the probe location while keeping the mutation constant allows us to look at the field at multiple locations in the protein while keeping the cause of the field constant. By then making a mutation and scanning across the surface of the protein again, we can see how well changes in the field due to a mutation are also calculated. This is the way data has previously been presented and is included for consistency.

The first important observation is that no single method stands out as the "best" field calculation method. There are cases in which AMOEBA, AMOEBA with intuitive charge penetration parameters (AMOEBA CP), and AMOEBA with fitted charge penetration parameters (AMOEBA CPf) all have the largest magnitude in correlation

(Rap E30/K31, Ral), cases in which AMOEBA with explicit solvent (with and without charge-penetration corrections) have the highest magnitude in correlation (Ras D30/E31K), APBS has the highest correlation magnitude (Rap E30D/K31, Rap E30D/K31E), and the hybrid TIP3P reaction field has the highest correlation magnitude (Rap E30/K31E, Ras D30E/E31K, Ras D30E/E31) and there are cases where each respective model has the lowest correlation magnitude. Furthermore, there is no consistent trend regarding the sign of the VSTR. In general, the VSTR is negative, although there are cases in each model where a positive value is calculated. The known Stark tuning rate is 1.99 $cm^{-1}/(k_bT/eÅ)$, and none of the methods yeild consistently positive. The direction of the correlation, and therefore sign of the VSTR, will be addressed further, but at this point it is sufficient to say that none of the models are consistently able to model the changes in fields due to changing locations of the probe with any significant degree of consistency.

One of the reasons for using AMOEBA was the inclusion of atomic polarizability, eliminating the need to select for a protein dielectric based on the observed VSTR. Put another way, we hypothesized that AMOEBA would do a better job at predicting a VSTR which matched the experiment Stark tuning rate. However, we observed that the average order of correct magnitudes was AMOEBA (CP, CPf) > APBS > hybrid TIP3P reaction field > 5 Å water sphere > experimental Stark tuning rate > AMOEBA explicit water (CP, CPf) > explicit TIP3P reaction field electrostatics. Implicit solvent AMOEBA was further from the experimental Stark tuning rate than implicit solvent Amber03 while explicit solvent AMOEBA was also further from the experimental Stark tuning rate than explicit TIP3P solvent in Amber03.

1.2.2 Electrostatic Fields at a Single Point on Ral

The advantage of looking at a single probe and making changes elsewhere in the system, while leaving the probe location constant, is we are able to see how the probe's

local field changes as a function of relatively distant residues without having to be concerned with changes due to the local environment, such as different degrees of solvent accessibility or hydrogen bonding. The probe and its immediate surroundings are relatively constant and the only changes being observed are on the binding partner.

Contrary to looking at a single GTPase and different probes, a single electrostatic method did consistently yield the highest (or close to) correlation to experimental measurement--APBS. The only exceptions are K32C and N54C, where the magnitude of the correlation is similar for PB as for the most correlated method, but the sign was opposite.

Once again, we look at how the magnitudes of the VSTR compare to the experimental Stark tuning rate, APBS > Hybrid > AMOEBA (CP, CPf) > experimental Stark tuning rate > 5 Å water sphere > explicit TIP3P reaction field electrostatics > AMOEBA explicit water (CP, CPf). In this, implicit solvent AMOEBA best predicted the magnitude of the Stark tuning rate. Because we are not looking at a single point in space and making changes elsewhere (rather than making changes at a single point in space and observing that one change from multiple perspectives), it was hypothesized that a single, uniform solute dielectric (and therefore VSTR) would be more appropriate. If a protein interior is not a uniform dielectric, then observing the same change at two different points can be complicated by varying amounts of charge screening between the changed potential and the observed field location. Observing changes from a single point, where the electrostatic field propagates along the same path to get from the mutation site to the measurement site, means the dielectric "path" should be constant. However, this whole discussion is moot because looking at the electrostatic fields from this perspective was typically worse in AMOEBA, the force field that should not care about a dielectric "path" because polarizability is explicitly modeled. In fact, AMOEBA typically did a significantly better job of predicting electrostatic fields at various points in space due to a single perturbation.

1.2.3 Changes in Field upon Docking

Previously we observed that looking at the difference field calculations typically yielded an improved correlation to experiment. Something non-physical about both sets of fields was cancelled out by looking at the difference between the two. Here, however, that observation is not universally true. Table 1-2 shows the relative field correlations and VSTR. Looking at fields calculated in APBS, correlation only increased significantly for Rap E30/K31 and Ras D30E/E31K (It is interesting to note that these two GTPases share amino acid identity at positions 30 and 31). In these two cases, looking at the change in field upon docking to the monomer, which had essentially zero correlation to experiment, significantly improved the correlation to experiment. For the other size GTPases, the difference calculation either decreased correlation or had no significant effect. Interestingly, the two GTPases that were improved by looking at the difference calculation, like the monomer, were poorly correlated to experiment in the absolute calculations, while the other six were already better correlated. It's likely that the reason for poor correlation in the absolute field calculations was similar for the monomer as Rap E30/K31 and Ras D30E/E31K, and thus taking the difference had the previously-observed effect of canceling out some error, while the other six GTPases either did not have that error, or had it to a significantly less degree, and by subtracting the monomer field it was introduced. For every other electrostatic method, the difference calculations did not have any systematic improvement on the correlation to experiment.

1.2.4 Overall Electrostatic Field Predictions Along Protein Surfaces

We want to know how well each model, overall, is capable of predicting the electrostatic field via the VSE. The last row of Table 1-1 shows the correlation coefficient and VSTR for each electrostatic method when all 54 systems are examined together. None of the AMOEBA methods are significantly correlated to experiment. APBS has the highest correlation (p-value = 0.0042), followed by the 5 Å water sphere

(0.0217). When taking the difference, the correlation increase for APBS (p-value < 0.0001), the hybrid TIP3P reaction field electrostatics (p-value = 0.0025). The explicit solvent AMOEBA (CP, CPf) calculations also saw an improved correlation, but the correlation is still too small to have likely statistical significance (p-values = 0.1430, 0.1878, 0.1471).

1.3 TIP3P WATER LOOKS LIKE PB IMPLICIT SOLVENT

We performed PB calculates on fixed orientations of two small molecules, methylthiocyanate and acetophenone, in various solvents (represented as only a dielectric constant in the PB model). We then compared them to experimental measurements of the vibrational absorbtion frequencies for methylthiocyanate in those solve, obtained by Christina Ragain, Ph.D, Josh Slocum, and Kelsey Eklund, and vibrational absorption frequencies previously reported by Fried *et al*,[1] shown in Figure 1-1. We observed that PB solvent is much better capable of predicting fields which follow the VSE in solvents which cannot hydrogen bond to the vibrational chromophore than in solvents which can. This is not a particularly surprising results--PB treats solvent as a continuum of dielectric and if there is a specific interaction between the solvent and the solute that cannot be well-represented by a continuum, it is neglected.

1.4 GENERAL REMARKS

With better solvent sampling, the 5 Å water sphere is no better than the purely implicit solvent. The most remarkable difference in the previous study was how well it improved the fields for the Ral monomers when grouped by probes, but no such improvement is observed.

The GROMACS explicit TIP3P reaction field electrostatic method was typically no better than APBS, and in some cases significantly worse (Ras D30E/E31). The hybrid TIP3P reaction field method typically looked very much like the APBS field (due to both

using the same solute fields), with the difference being the implicit PB SRF is used for the APBS results while the explicit TIP3P solvent reaction field is used for the hybrid method. The general agreement between the two is due to the approximately 1:1 relationship between the two solvent reaction fields, as previously discussed and shown in Figure 1-3.

The charge-penetration corrections were not significantly different from the AMOEBA fields without charge-penetration. Due to 1) the short-range nature of the correction and 2) that the local structural environment was, on average, the same for a probe docked to each GTPase, the average of the charge-penetration correction field was approximately constant, resulting in a uniform shift for all field calculations and no overall change in correlation. It should be noted that the current state of the charge-penetration corrections treat add them after the self-consistent induced dipole calculations, and it may be that further development within the procedure, including using the charge-penetration corrected fields when calculating self-consistent induced dipoles and expanding the corrections from just monopole-monopole interaction to dipole-dipole and quadrupole-quadrupole, may merit reassessment of their usefulness.

Correlations between the calculated standard deviation of the electrostatic field using the various field calculation methods and the experimental full width at half peak maximum are shown in Table 1-3. In general, there is little-to-no correlation between the two. When a statistically significant correlation is observed (p-value <= 0.10: R > 0. 72 for N=6, R>0.58 for N=9, R> 0.23 for N=54), the correlation is negative, indicating that more electrostatic field states results in a narrower vibrational absorption peak and fewer electrostatic field states results in a broader vibrational absorption peak. However, we would expect the opposite trend--broader absorption peaks should be indicative of a larger number of states which would manifest itself in simulation as a broader array of electrostatic field environment, and thus it's likely that the significantly correlated cases may actually be random noise.

It's also highly likely that AMOEBA underperforms due to a non-transferability among ensembles. In the next study, we will examine a few significantly smaller systems which have been sampled in AMOEBA.

Table 1-1: Correlation Coefficients (R) and Virtual Stark Tuning Rates (VSTR[a]) for Absolute Field Calculations using Various Electrostatic Models

F vs. $\tilde{\nu}$	AMOEBA		AMOEBA CP		AMOEBA CPf		AMOEBA Explicit Water		AMOEBA Explicit Water CP		AMOEBA Explicit Water CPf	
	R	VSTR	R	VSTR	R	VSTR	R	VSTR	R	VSTR	R	VSTR
Rap E30/K31	0.581	0.112	0.578	0.107	0.581	0.112	-0.165	-0.773	-0.188	-0.639	-0.168	-0.751
Rap E30/K31E	-0.316	-0.613	-0.267	-0.737	-0.314	-0.619	-0.192	-4.670	-0.223	-3.793	-0.196	-4.573
Rap E30D/K31	-0.846	-0.306	-0.838	-0.303	-0.845	-0.305	-0.279	-3.764	-0.354	-2.742	-0.284	-3.680
Rap E30D/K31E	-0.819	-0.221	-0.812	-0.220	-0.819	-0.221	-0.558	-1.166	-0.568	-1.031	-0.560	-1.148
Ras D30E/E31K	0.072	3.230	-0.013	-16.500	0.069	3.367	0.313	0.938	0.278	1.031	0.311	0.941
Ras D30E/E31	-0.614	-0.513	-0.572	-0.483	-0.612	-0.511	0.162	1.408	0.126	1.682	0.160	1.419
Ras D30/E31K	-0.308	-0.286	-0.265	-0.339	-0.307	-0.286	-0.926	-0.107	-0.927	-0.100	-0.925	-0.107
Ras D30/E31	0.604	0.241	0.626	0.228	0.605	0.241	-0.302	-1.001	-0.304	-0.919	-0.305	-0.984
Ral	0.380	0.521	0.442	0.452	0.384	0.516	0.090	3.992	0.070	5.013	0.087	4.142
N27C$_{SCN}$	0.016	2.817	0.001	73.333	0.015	2.857	0.141	0.456	0.133	0.452	0.140	0.454
G28C$_{SCN}$	-0.422	-0.561	-0.403	-0.537	-0.421	-0.560	-0.260	-0.948	-0.294	-0.766	-0.263	-0.932
N29C$_{SCN}$	-0.295	-0.191	-0.272	-0.194	-0.294	-0.191	0.091	0.759	0.085	0.750	0.090	0.760
Y31C$_{SCN}$	-0.288	-0.541	-0.290	-0.524	-0.288	-0.540	-0.033	-13.750	-0.005	-76.154	-0.030	-15.231
K32C$_{SCN}$	-0.165	-0.746	-0.163	-0.715	-0.164	-0.746	0.385	0.661	0.370	0.649	0.383	0.660
N54C$_{SCN}$	-0.204	-0.481	-0.200	-0.470	-0.204	-0.481	0.085	2.857	0.096	2.391	0.086	2.793
All Points	-0.106	-1.380	-0.096	-1.463	-0.106	-1.383	-0.032	-7.279	-0.050	-4.361	-0.034	-6.851
	APBS		APBS 5 ÅSphere		GROMACS TIP3P Reaction Field		Hybrid TI3P Reaction Field					
	R	VSTR	R	VSTR	R	VSTR	R	VSTR				
Rap E30/K31	-0.128	-1.252	-0.206	-0.970	-0.427	-0.416	-0.075	-1.800				
Rap E30/K31E	-0.659	-0.280	-0.646	-0.380	-0.293	-1.870	-0.739	-0.301				
Rap E30D/K31	-0.892	-0.301	-0.862	-0.453	-0.884	-0.813	-0.815	-0.503				
Rap E30D/K31E	-0.875	-0.205	-0.841	-0.280	-0.366	-1.338	-0.740	-0.326				
Ras D30E/E31K	0.203	2.340	0.112	3.542	0.174	1.840	0.494	0.602				
Ras D30E/E31	-0.599	-0.650	-0.527	-0.886	-0.073	-5.252	-0.718	-0.461				
Ras D30/E31K	-0.709	-0.135	-0.792	-0.119	-0.866	-0.129	-0.494	-0.157				
Ras D30/E31	0.620	0.332	0.471	0.544	-0.136	-4.000	0.781	0.207				
Ral	-0.191	-1.776	-0.031	-13.113	0.053	12.073	-0.345	-0.902				
N27C$_{SCN}$	0.405	0.230	0.399	0.300	0.283	0.306	0.422	0.277				
G28C$_{SCN}$	-0.816	-0.349	-0.694	-0.472	-0.376	-0.987	-0.758	-0.443				
N29C$_{SCN}$	-0.359	-0.216	-0.220	-0.379	-0.059	-1.383	-0.328	-0.239				
Y31C$_{SCN}$	-0.523	-0.438	-0.338	-0.805	-0.332	-1.085	-0.368	-0.666				
K32C$_{SCN}$	-0.320	-1.694	0.052	8.800	0.339	0.776	0.053	6.286				
N54C$_{SCN}$	-0.178	-0.668	-0.142	-1.010	-0.051	-6.326	0.270	0.739				
All Points	-0.384	-0.568	-0.312	-0.808	-0.159	-1.795	-0.211	-1.008				

[a]VSTR has units of $cm^{-1}/(k_bT/eÅ)$. The known VSTR is 1.99 $cm^{-1}/(k_bT/eÅ)$.

Table 1-2: Correlation Coefficients (R) and Virtual Stark Tuning Rates (VSTR[a]) for Relative Field Calculations using Various Electrostatic Models

ΔF vs. $\Delta\tilde{\nu}$	AMOEBA		AMOEBA CP		AMOEBA CPf		AMOEBA Explicit Water		AMOEBA Explicit Water CP		AMOEBA Explicit Water CPf	
	R	VSTR	R	VSTR	R	VSTR	R	VSTR	R	VSTR	R	VSTR
Rap E30/K31	-0.469	-0.200	-0.467	-0.198	-0.469	-0.200	0.840	0.256	0.834	0.249	0.838	0.255
Rap E30/K31E	-0.019	-14.776	0.028	10.312	-0.016	-17.522	0.283	1.359	0.265	1.396	0.280	1.366
Rap E30D/K31	-0.052	-8.722	-0.016	-27.887	-0.050	-9.000	-0.046	-10.421	-0.100	-4.648	-0.051	-9.384
Rap E30D/K31E	0.218	1.002	0.225	0.965	0.220	0.993	0.897	0.456	0.876	0.449	0.896	0.456
Ras D30E/E31K	0.126	0.923	0.132	0.823	0.128	0.906	-0.036	-6.246	-0.062	-3.449	-0.037	-6.000
Ras D30E/E31	0.612	0.072	0.574	0.072	0.609	0.073	0.432	0.132	0.426	0.126	0.431	0.132
Ras D30/E31K	0.311	0.743	0.382	0.646	0.316	0.732	0.171	1.187	0.129	1.472	0.169	1.197
Ras D30/E31	0.651	0.477	0.721	0.410	0.655	0.473	0.021	12.000	0.028	8.426	0.020	12.375
All Points	0.016	0.204	0.034	0.454	0.018	0.223	0.202	1.777	0.182	1.710	0.200	1.769

	APBS		APBS 5 ÅSphere		GROMACS TIP3P Reaction Field		Hybrid TI3P Reaction Field	
	R	VSTR	R	VSTR	R	VSTR	R	VSTR
Rap E30/K31	-0.973	-0.196	-0.481	-0.680	0.299	1.171	-0.699	-0.284
Rap E30/K31E	-0.688	-0.272	-0.529	-0.511	-0.010	-41.250	-0.663	-0.348
Rap E30D/K31	-0.728	-0.351	-0.690	-0.634	-0.434	-1.464	-0.797	-0.543
Rap E30D/K31E	-0.387	-0.513	-0.177	-1.930	0.789	0.621	-0.328	-1.427
Ras D30E/E31K	-0.604	-0.589	-0.175	-1.909	0.092	3.183	-0.134	-2.000
Ras D30E/E31	0.264	0.366	0.445	0.445	0.210	0.556	-0.093	-2.134
Ras D30/E31K	-0.393	-0.515	0.015	14.887	0.064	4.231	-0.359	-0.546
Ras D30/E31	-0.265	-1.128	0.136	3.328	-0.288	-1.674	0.098	2.773
All Points	-0.549	-5.224	-0.278	-1.945	0.018	0.115	-0.403	-3.204

[a]VSTR has units of $cm^{-1}/(k_bT/eÅ)$. The known VSTR is 1.99 $cm^{-1}/(k_bT/eÅ)$.

Table 1-3: Correlation Coefficients for Field Standard Deviations Compared to Experimental Full Width at Half Peak Maximum (FWHM) using Various Electrostatic Methods

Fits/Mutant	AMOEBA	AMOEBA CP	AMOEBA CPf	AMOEBA Explicit Water	AMOEBA Explicit Water CP	AMOEBA Explicit Water CPf
Rap E30/K31	-0.571	-0.571	-0.571	-0.754	-0.753	-0.754
Rap E30/K31E	0.159	0.158	0.159	-0.456	-0.446	-0.456
Rap E30D/K31	0.073	0.073	0.073	-0.796	-0.804	-0.796
Rap E30D/K31E	-0.294	-0.297	-0.294	-0.328	-0.330	-0.328
Ras D30E/E31K	-0.058	-0.058	-0.058	0.400	0.402	0.400
Ras D30E/E31	-0.324	-0.322	-0.324	-0.075	-0.057	-0.075
Ras D30/E31K	0.634	0.633	0.634	-0.062	-0.062	-0.062
Ras D30/E31	-0.348	-0.348	-0.348	0.006	0.002	0.006
$N27C_{SCN}$	0.110	0.109	0.110	0.251	0.253	0.251
$G28C_{SCN}$	0.348	0.348	0.348	0.573	0.574	0.573
$N29C_{SCN}$	-0.605	-0.605	-0.605	-0.815	-0.816	-0.815
$Y31C_{SCN}$	0.111	0.111	0.111	0.025	0.030	0.025
$K32C_{SCN}$	-0.130	-0.129	-0.130	-0.277	-0.276	-0.277
$N54C_{SCN}$	0.249	0.247	0.249	0.064	0.062	0.064
All Points	-0.125	-0.125	-0.125	-0.139	-0.137	-0.139

	APBS	APBS 5 ÅSphere	GROMACS TIP3P Reaction Field	Hybrid TI3P Reaction Field
Rap E30/K31	-0.666	-0.675	-0.641	-0.741
Rap E30/K31E	-0.077	0.371	0.167	-0.296
Rap E30D/K31	-0.103	-0.352	-0.537	-0.209
Rap E30D/K31E	-0.485	-0.586	-0.274	-0.525
Ras D30E/E31K	0.057	0.281	0.297	0.157
Ras D30E/E31	-0.414	-0.408	-0.047	-0.413
Ras D30/E31K	0.550	0.718	0.164	0.441
Ras D30/E31	-0.594	-0.384	-0.127	-0.746
$N27C_{SCN}$	0.107	0.221	0.191	0.173
$G28C_{SCN}$	0.383	0.298	0.262	0.434
$N29C_{SCN}$	-0.536	-0.748	-0.880	-0.547
$Y31C_{SCN}$	0.024	0.296	0.527	0.031
$K32C_{SCN}$	-0.287	-0.264	-0.453	-0.199
$N54C_{SCN}$	0.261	0.321	0.049	0.304
All Points	-0.189	-0.136	-0.118	-0.235

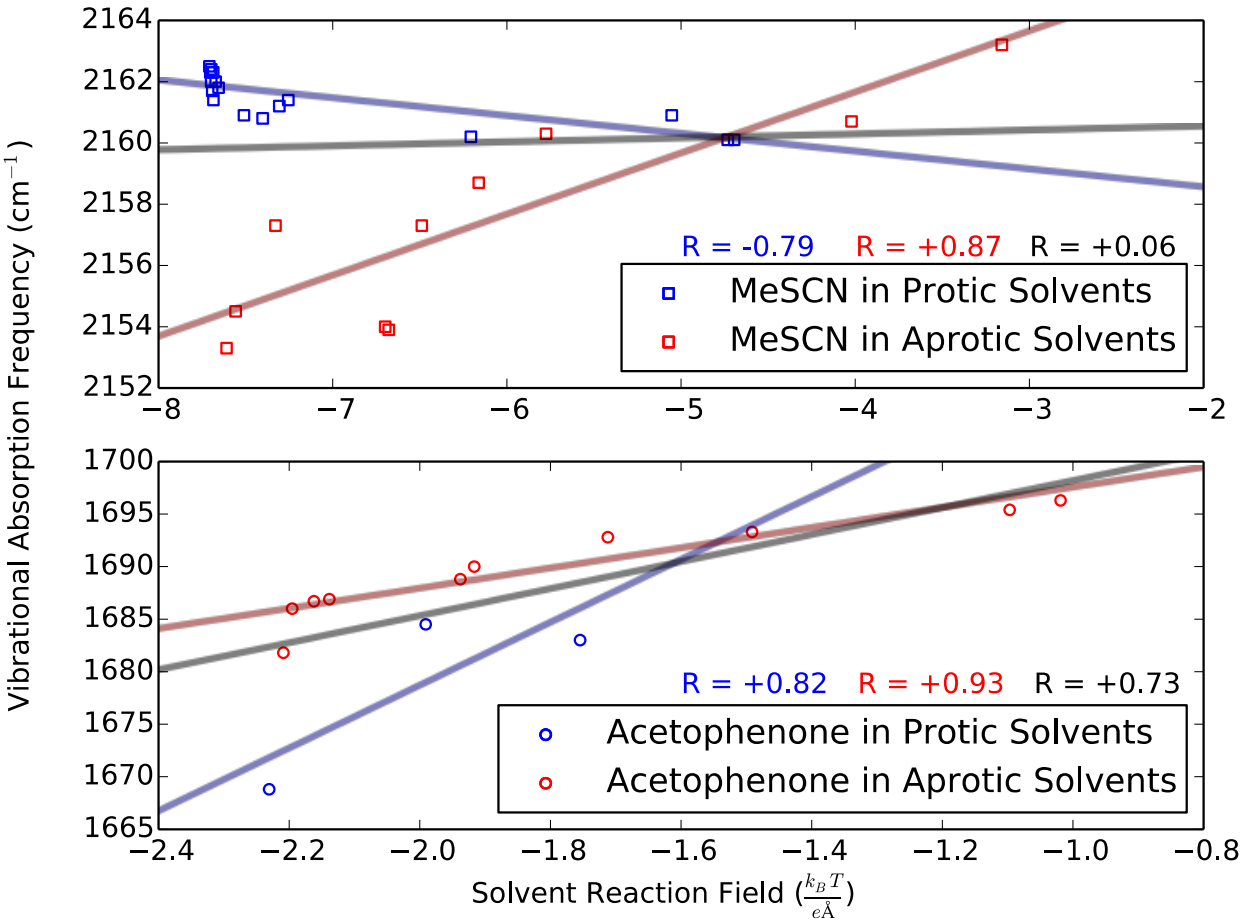

Figure 1-1: Poisson-Boltzmann Solvent Reaction Fields for Methylthiocyanate and Acetophenone in Various Solvents

Solvent Reaction Fields on (top) methylthiocyanate and (bottom) acetophenone calculated using APBS where each solvent is described as a dielectric continuum. Blue: solvents which can donate a hydrogen bond to the vibrational chromophore; red: solvent which cannot hydrogen bond to the vibrational chromophore. Best fit lines and correlations coefficients are included, with black being the aggregate of all data points. Experimental measurements for methylthiocyanate are unpublished were performed by Christina Ragain, Ph.D., Josh Slocum, and Kelsey Eklund. Experimental measurements for acetophenone were previously reported by Fried *et al.*[1]

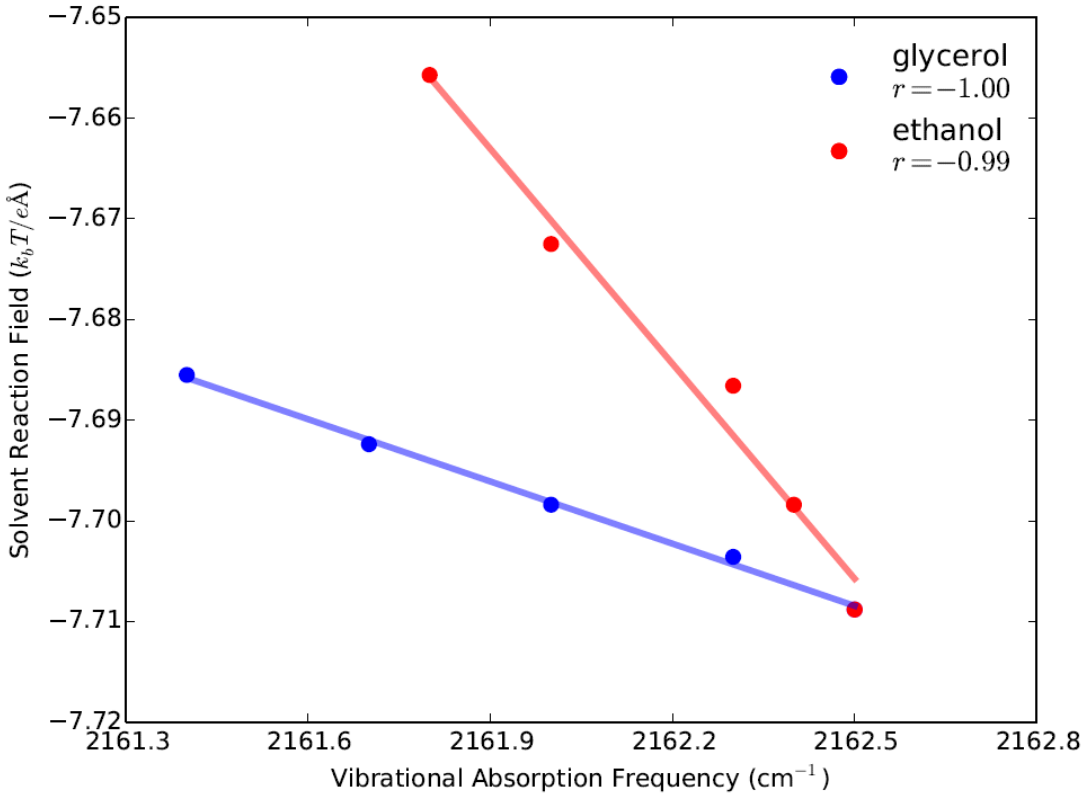

Figure 1-2: Methylthiocyanate Solvent Reaction Fields at Various Dielectrics, Modulated by Glycerol and Ethanol

The solvent reaction field calculated in APBS for methylthiocyanate at various dielectrics. (Red) Dielectric constant was modulated by addition of glycerol. (Blue) Dielectric constant was modulated by addition of ethanol.

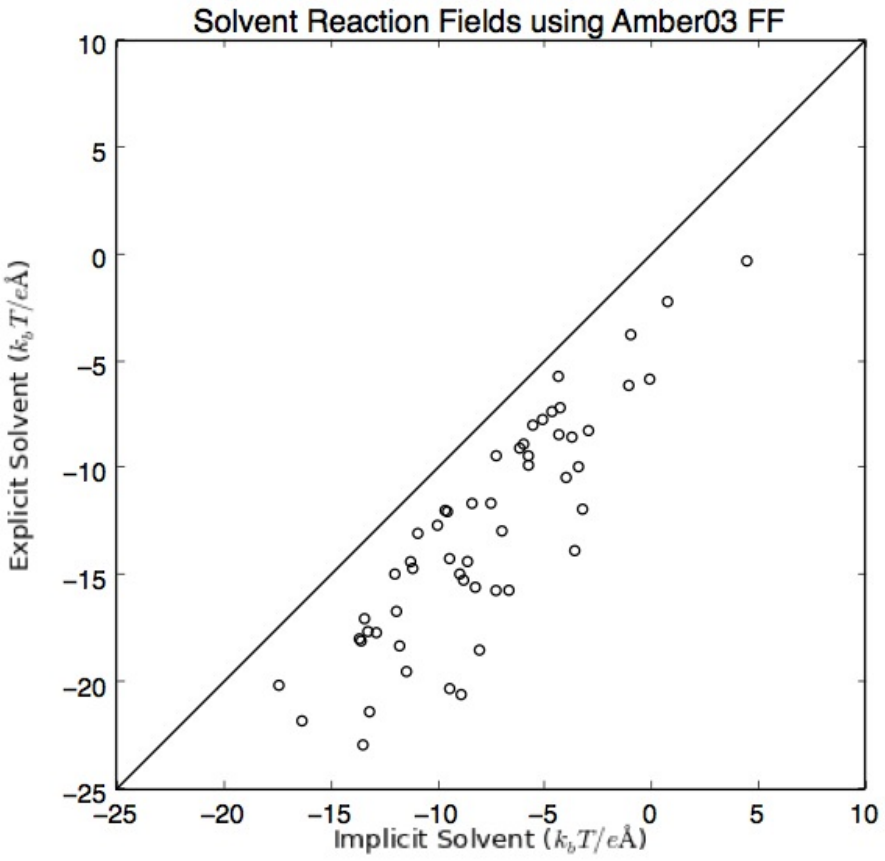

Figure 1-3: Comparison Between Solvent Reaction Fields Calculated using Explicit TI3P Water and Implicit PB Water for All 54 GTPase/Ral Probe Combinations

The solvent reaction fields using explicit TIP3P water plotted against the solvent reaction fields using implicit PB water with Amber03 point charges for all explicitly defined atoms. The line along y=x is not a best fit line and is meant to show that the two models are 1:1 with the implicit solvent being consistently less negative.

(1) Fried, S. D.; Bagchi, S.; Boxer, S. G. *J Am Chem Soc* **2013**, *135*, 11181.